

**Electron capture by  $\text{Ne}^{3+}$  ions from atomic hydrogen**R. Rejoub,\* M. E. Bannister,<sup>†</sup> and C. C. Havener<sup>‡</sup>*Physics Division, Oak Ridge National Laboratory, Oak Ridge, Tennessee 37831-6372, USA*D. W. Savin<sup>§</sup>*Columbia Astrophysics Laboratory, Columbia University, New York, New York 10027-6601, USA*C. J. Verzani<sup>||</sup>*J. R. Macdonald Laboratory, Department of Physics, Kansas State University, Manhattan, Kansas 66506-2604, USA*J. G. Wang<sup>¶</sup> and P. C. Stancil<sup>\*\*</sup>*Department of Physics and Astronomy and the Center for Simulational Physics, The University of Georgia, Athens, Georgia 30602-2451, USA*

(Received 14 November 2003; revised manuscript received 6 January 2004; published 10 May 2004)

Using the Oak Ridge National Laboratory ion-atom merged-beam apparatus, absolute total electron-capture cross sections have been measured for collisions of  $\text{Ne}^{3+}$  ions with hydrogen (deuterium) atoms at energies between 0.07 and 826 eV/u. Comparison to previous measurements shows large discrepancies between 50 and 400 eV/u. Previously published molecular-orbital close-coupling (MOCC) calculations were performed over limited energy ranges, but show good agreement with the present measurements. Here MOCC calculations are presented for energies between 0.01 and 1000 eV/u for collisions with both H and D. For energies below  $\sim 1$  eV/u, an enhancement in the magnitude of both the experimental and theoretical cross sections is observed which is attributed to the ion-induced dipole attraction between the reactants. Below  $\sim 4$  eV/u, the present calculations show a significant target isotope effect.

DOI: 10.1103/PhysRevA.69.052704

PACS number(s): 34.70.+e, 34.80.Kw

**I. INTRODUCTION**

Qualitative and quantitative knowledge of the physics of charge-changing collisional processes is fundamental to the understanding of the behavior of a wide range of plasmas. Electron capture (EC) by multicharged ions from a neutral atom is one such process. The present investigation was motivated, in part, by applications in astrophysics and for impurity control in thermonuclear plasmas [1] where electron capture has a dominating influence on the ionization balance.

In fusion energy research, EC cross sections for energies between  $\sim 1$  and  $\sim 100$  eV/u are needed for accurate modeling and diagnostics of the scrape-off layer (i.e., edge) plasma. An issue of particular interest is the effect that impurity ions have on fusion plasmas. For example, impurity effects have been studied by injection of Ne into the DIII-D device, the third-generation tokamak developed by General Atomics in San Diego, CA. The subsequent radiation, as the highly charged Ne ions underwent EC with atomic hydrogen,

reduced the heat flux to the plasma facing surfaces [2]. Accurate modeling of the Ne charge balance and radiative cooling in these plasmas requires reliable EC cross-section data for a wide range of energies and Ne ionization stages.

In astrophysics, EC cross sections are important in planetary nebulae with hot central stars where the large number of stellar photons with energies well above the H I ionization limit (where the photoionization cross section is low) results in a significant fraction of H in the nebula being neutral [3]. Special attention has been paid to the Ne III lines with radiative transitions at 2590 and 2678 Å, with upper levels corresponding to the  $2p^3 3p^5 P$  and  $2p^3 3p^3 P$  excited states of  $\text{Ne}^{2+}$ , respectively. These states are the dominant levels populated in the charge-exchange reaction of  $\text{Ne}^{3+}$  with H [4]. Such emission lines are used as diagnostics and to infer the elemental abundances in the nebula [5,6].

Despite the importance of low-energy electron capture for  $\text{Ne}^{3+} + \text{H}$ , there has been no systematic experimental study of this collision system. Previously measured cross sections performed by Huber [7] and Can *et al.* [8] at relatively high energies (i.e., above 60 eV/u) indicate a decreasing cross section toward lower energies, but show a large discrepancy with the earlier measurements of Seim *et al.* [9] around 400 eV/u. A decreasing trend is in poor agreement with the multichannel Landau-Zener (MCLZ) calculations of Wilson *et al.* [10] which were used to normalize their state-selective measurements [10].

Molecular-orbital close-coupling (MOCC) calculations are considered most appropriate for the low-energy collisions relevant to astrophysical environments, but require considerable effort. There exist two previous MOCC calculations, but

\*Electronic address: [alrejoubra@ornl.gov](mailto:alrejoubra@ornl.gov)<sup>†</sup>Electronic address: [bannisterme@ornl.gov](mailto:bannisterme@ornl.gov)<sup>‡</sup>Electronic address: [havenercc@ornl.gov](mailto:havenercc@ornl.gov)<sup>§</sup>Electronic address: [savin@astro.columbia.edu](mailto:savin@astro.columbia.edu)<sup>||</sup>Electronic address: [cverzani@nist.gov](mailto:cverzani@nist.gov)<sup>¶</sup>Present address: Institute of Applied Physics and Computational Mathematics, P. O. Box 8009, Beijing 100089, P. R. China. Electronic address: [wang\\_jianguo@mail.iapcm.ac.cn](mailto:wang_jianguo@mail.iapcm.ac.cn)<sup>\*\*</sup>Electronic address: [stancil@physast.uga.edu](mailto:stancil@physast.uga.edu)

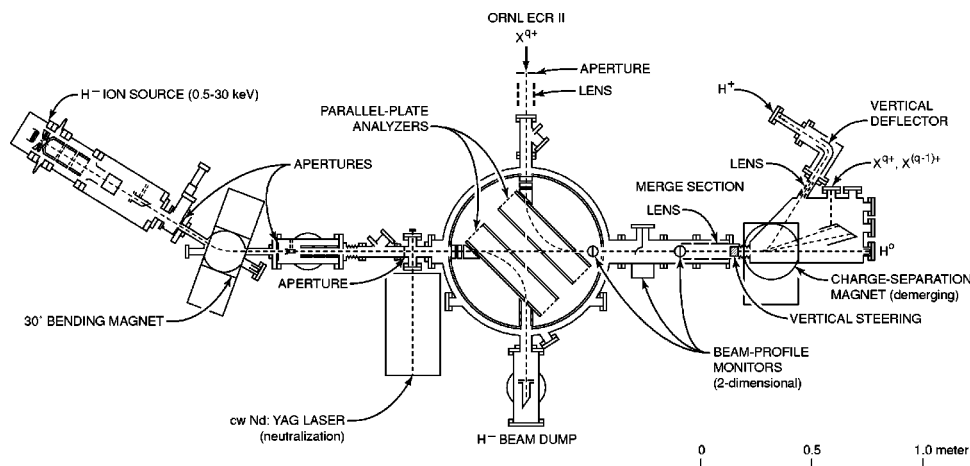
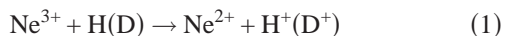


FIG. 1. Schematic of the ion-atom merged-beam apparatus.

for limited energy ranges. The MOCC calculations of Gargaud and McCarroll [11] show large discrepancies with the previous experimental results of Huber [7] and Can *et al.* [8] between 60 and 400 eV/u. Earlier MOCC calculations by Heil *et al.* [12] between 0.3 and 8.4 eV/u show a flat low-energy cross section, in agreement with the trend of the Gargaud and McCarroll results.

At the low collision energies of interest here, the ion-induced dipole potential between reactants is important. The attractive force due to this potential, and the resulting acceleration of the particles toward each other, significantly modify the reactant trajectories. This results in the incident trajectories accessing internuclear distances smaller than the initial impact parameter. At low enough energies, these trajectory effects can dominate the electron transfer process and lead to enhanced cross sections [13]. Several systems have been investigated using the ORNL merged-beam apparatus and show such enhancements [14]. Ion-induced dipole enhancements also lead to significant target isotope effects [15,16].

A systematic experimental and theoretical study of the low-energy electron-capture process



is presented here. The absolute electron-capture cross section was measured with ground-state deuterium at collision energies from 0.07 to 826 eV/u using a merged-beam technique. The metastable fraction of the  $\text{Ne}^{3+}$  beam was measured using electron-impact ionization. MOCC and MCLZ calculations for collisions with hydrogen and deuterium have been obtained over the energy range of 0.01–1000 eV/u. Additionally, MCLZ calculations for metastable states of  $\text{Ne}^{3+}$  have been carried out.

## II. EXPERIMENTAL APPROACH

### A. Merged-beam technique

The measurement of the EC cross section for the  $\text{Ne}^{3+} + \text{H}(\text{D})$  system was performed using the ORNL ion-atom merged-beam apparatus. In merged beams, relatively fast

(keV) beams are merged producing a large dynamic range of collision energies in the center of mass [17]. In the present investigation, a  $\text{Ne}^{3+}$  beam with energies of 51–66 keV is merged with a faster D beam at energies of 7 keV and 8 keV, allowing center-of-mass collision energies in the range of 0.07–826 eV/u. The apparatus is depicted schematically in Fig. 1 and has previously been described in detail [14,17].

As depicted in Fig. 1, a neutral ground-state D atom beam is obtained by photodetachment of a  $\text{D}^-$  beam as it crosses the optical cavity of a 1.06  $\mu\text{m}$  cw Nd:YAG (Yttrium aluminum garnet) laser where kilowatts of continuous power circulate. The  $\text{D}^-$  beam is extracted from a duoplasmatron source. Collisional detachment of the  $\text{D}^-$  beam on background gas results in a small fraction (0.01%) of excited states in the D beam. The obtained D beam is nearly parallel (the divergence being less than  $0.15^\circ$ ) with a beam diameter of 2 mm and intensities ranging from 10 to 20 nA. Deuterium is used instead of hydrogen to maximize the angular acceptance of the  $\text{H}^+(\text{D}^+)$  detector [17,18].

A  $\text{Ne}^{3+}$  beam is electrostatically merged with the neutral D beam (see Fig. 1). The  $\text{Ne}^{3+}$  beam is produced by the ORNL CAPRICE ECR ion source [19] with an intensity of  $\approx 4 \mu\text{A}$ , a diameter of 2–4 mm (full width at half maximum) and a divergence less than  $0.25^\circ$ . The purity of the  $\text{Ne}^{3+}$  beam with respect to metastable states is discussed in Sec. II B. Both beams interact along a field-free region of 47 cm, after which the  $\text{D}^+$  product ions are magnetically separated from the primary beams. The merge path is maintained under ultrahigh vacuum conditions to minimize the  $\text{D}^+$  background generated by stripping of the D beam as it travels through the background gas. To maximize the angular acceptance of  $\text{D}^+$ , a cylindrical Einzel lens is placed near the end of the merge path. Due to limited magnetic dispersion, the heavy product of the reaction,  $\text{Ne}^{2+}$ , is not measured but is collected along with the primary ion beam,  $\text{Ne}^{3+}$ , in a large Faraday cup. Since only the  $\text{D}^+$  signal is measured, the apparatus actually measures electron loss, the sum of electron capture and ionization. However, ionization at these energies is negligible compared to electron capture. The D neutral beam is monitored by measuring secondary emission from a

stainless-steel plate. The product signal D<sup>+</sup> ions are detected by a channel electron multiplier. The signal rate (hertz) is extracted from the background (kilohertz) by a two-beam modulation technique [17]. To correct the signal rate for the small fraction of excited D, the signal is measured with and without the laser on. The difference between the signals corresponded to the signal due to the D ground-state collisions.

The absolute electron-capture cross section is determined at each velocity from directly measurable parameters by the following formula:

$$\sigma = \frac{R\gamma q e^2 v_1 v_2}{I_1 I_2 v_r L \langle F \rangle}, \quad (2)$$

where  $R$  is the signal count rate,  $q$  the charge of ion,  $e$  the electronic charge,  $I_1$  and  $I_2$  the intensities of the two beams,  $v_1$  and  $v_2$  are the velocities of the beams,  $v_r$  the relative velocity between beams,  $L$ , the merge-path length,  $\gamma$  the secondary electron emission of the neutral detector, and  $\langle F \rangle$  the average form factor, which is a measure of the overlap of the two beams. The form factor is determined from two-dimensional measurements of the overlap of the two beams at three different positions along the merge path. The secondary electron emission coefficient  $\gamma$  is measured *in situ* as described previously [17] and found to range from 1.15 for 7 keV D<sup>-</sup> to 1.36 for 8 keV D<sup>-</sup>. The velocities  $v_1$  and  $v_2$  are calculated from the energies of the beams, which include the estimated plasma potential shifts of the two sources. The relative velocity  $v_r$  is calculated from the velocities of the beams and the measured merge angle between the beams for energies less than 1 eV/u (see, e.g., Ref. [15]).

### B. Ne<sup>3+</sup> beam purity

The cross section for capture onto a metastable ion can differ significantly from capture onto an ion in the ground state (see, for example, Ref. [20]). In order to investigate the fraction of metastables in the Ne<sup>3+</sup> ion beam produced by the ORNL ECR source, the beam, under similar ion source conditions, was directed to the crossed-beam apparatus [21,22] to measure electron-impact ionization. The measured ionization cross section (see Fig. 2) shows a small rise at energies below the threshold of 97.11 eV [23] for the Ne<sup>3+</sup> ( $2s^2 2p^3 \ ^4S^o$ ) ground state. This initial rise is attributed to ionization of Ne<sup>3+</sup> ( $2s^2 2p^3 \ ^2P^o$ ,  $^2D^o$ ) metastable ions in the beam with ionization thresholds of 89.4 eV and 92.03 eV, respectively [23]. Assuming that the ionization of Ne<sup>3+</sup> is dominated by direct processes, the semiempirical Lotz formula [24] can be used to represent individually the energy dependence of the ionization of the metastable and ground-state ions [25]. A least-squares fit to the experimental data (see Fig. 2) yields a ground-state fraction of  $0.94 \pm 0.03$  for the Ne<sup>3+</sup> ion beam. Estimates of the EC cross sections for the Ne<sup>3+</sup> metastables are obtained with the MCLZ method and are discussed below.

### III. THEORETICAL APPROACH

Single-electron capture for collisions of Ne<sup>3+</sup> with atomic hydrogen has been investigated within the molecular-orbital

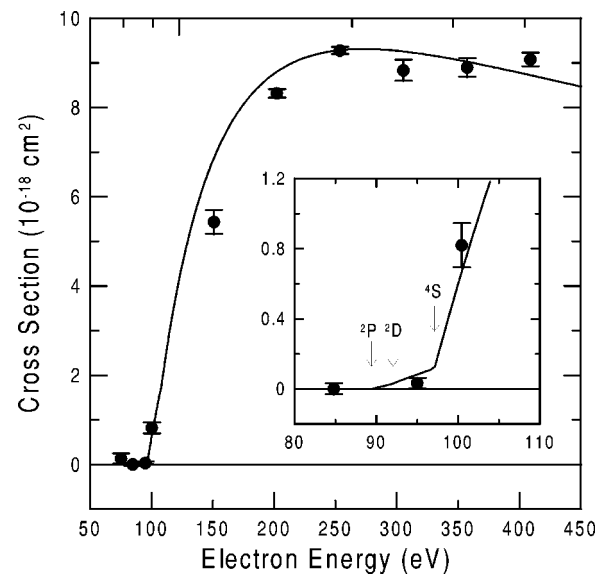


FIG. 2. Electron-ion cross-beam measurements of the electron-impact ionization cross section for  $e + \text{Ne}^{3+} \rightarrow \text{Ne}^{4+} + 2e$  as a function of the electron collision energy. Lotz fits to the data (solid lines) above and below threshold give the fraction of metastables in the Ne<sup>3+</sup> ion beam (see text for details).

picture using two quantum-mechanical approaches: the MOCC and the MCLZ approximation. We describe below pertinent details related to these calculations for this collision system.

#### A. Molecular-orbital close-coupling calculations

The quantum-mechanical MOCC method, which we only briefly discuss here, has been described thoroughly in the literature (e.g., Kimura and Lane [26], Zygelman *et al.* [27]). A coupled set of second-order differential equations is integrated using the log-derivative method of Johnson [28]. The  $S$  matrix is computed using a truncated set of (diabatic) molecular eigenfunctions, corresponding to the relevant open scattering channels, and a partial-wave expansion. The charge-transfer cross sections are then obtained from the appropriate  $S$ -matrix elements. Transitions between the scattering channels are induced by both radial and rotational nonadiabatic coupling matrix elements. In this work we include only the radial couplings. Rotational coupling is believed to be unimportant for the energy range considered.

We adopted the *ab initio* diabatic diagonal potentials and diabatic coupling matrix elements from Heil *et al.* [12], which were digitalized directly from figures in their paper. The separated atoms of the initial channel, Ne<sup>3+</sup>( $2p^3 \ ^4S^o$ ) + H( $1s \ ^2S$ ), correlate to the two molecular states  $^3\Sigma^-$  and  $^5\Sigma^-$  with approach probability factors of 3/8 and 5/8, respectively. For the  $^3\Sigma^-$  states, we included three charge-transfer channels, Ne<sup>2+</sup>( $2p^3 3s \ ^3S^o$ ) + H<sup>+</sup>, Ne<sup>2+</sup>( $2p^3 3p \ ^3P$ ) + H<sup>+</sup>, and Ne<sup>2+</sup>( $2p^3 3p \ ^3D^o$ ) + H<sup>+</sup>, resulting in a four-channel MOCC calculation. For the  $^5\Sigma^-$  states, two charge-transfer channels, Ne<sup>2+</sup>( $2p^3 3s \ ^5S^o$ ) + H<sup>+</sup> and Ne<sup>2+</sup>( $2p^3 3s \ ^5P$ ) + H<sup>+</sup>, were included giving a three-channel MOCC calculation. Neglect of rotational coupling will result in an underestimation of cap-

ture to  $\text{Ne}^{2+}(2p^3 3p \ ^3P)$ ,  $\text{Ne}^{2+}(2p^3 3s \ ^3D^o)$ , and  $\text{Ne}^{2+}(2p^3 3p \ ^5P)$ , but only at the highest energies considered. Electron translation factors (ETFs) are not considered as they are only expected to be relevant for collision energies above 1–5 keV/u. The combined uncertainty introduced with the neglect of rotational coupling and ETFs is on the order of 20% for  $E > 100$  eV/u, but considerably less for smaller collision energies. The errors introduced in the digitization of the diabatic potentials and couplings are expected to be more significant.

The kinematic target isotope effect [15,16] was also investigated by replacing the  $\text{Ne}^{3+}-\text{H}$  reduced mass with that of  $\text{Ne}^{3+}-\text{D}$  in the MOCC calculations. Isotope effects on the potentials and couplings, i.e., the shift in the center of mass, or the D ionization potential were not included, but their effects are expected to be small.

### B. Multichannel Landau-Zener calculations

MCLZ calculations were performed following the prescription of Butler and Dalgarno [29], including the H static dipole polarizability in the radial velocity relation, and the multichannel probability from the formulation of Janev *et al.* [30]. Empirical potentials and couplings were determined following Butler and Dalgarno. Cross sections were calculated for the ground  $\text{Ne}^{3+}(2p^3 \ ^4S^o)$  state for the same sets of channels as used in the MOCC computations. In addition, MCLZ calculations were performed for collisions of the  $\text{Ne}^{3+}(2p^3 \ ^2P^o)$  and  $\text{Ne}^{3+}(2p^3 \ ^2D^o)$  metastable ions with ground-state H. The MCLZ calculations for the  $^2P^o$  and  $^2D^o$  metastables included four and six spin-symmetry manifolds for a total of 21 and 26 electron-capture channels, respectively. All MCLZ calculations were repeated for the D target.

## IV. RESULTS AND DISCUSSION

Table I lists the measured absolute total EC cross section for  $\text{Ne}^{3+}+\text{D}$  as a function of collision energy. The statistical and total uncertainties are estimated at the 90% confidence level. The total uncertainty corresponds to a quadrature sum of the statistical and systematic errors. The total uncertainty includes an estimated uncertainty of 6% (added in quadrature) due to the observed presence of metastable ions in the  $\text{Ne}^{3+}$  beam and the MCLZ estimates for the metastable cross section (see below). No correction was made to the cross section due to the (6%) metastable ions. For energies less than 1 eV/u, the uncertainty in center-of-mass collision energy due to the energy spread of the D and  $\text{Ne}^{3+}$  beam and the spread in the merge angle is also shown. Figure 3 compares the measured cross sections to the present MOCC and MCLZ calculations and previous theory and experiment. While Fig. 3 shows the present measurements to be in agreement with the results of Seim *et al.* [9], there is significant discrepancy with the measurements of Can *et al.* [8] and Huber [7], both of which suggest that the cross section decreases with decreasing energy. All three previous measurements relied on a hydrogen target created by dissociation of molecular hydrogen. This technique can lead to normalization problems (e.g., see Ref. [31]). Further, it is not known if

TABLE I. Ion-atom merged-beam cross-section data for  $\text{Ne}^{3+}+\text{H}(\text{D})\rightarrow\text{Ne}^{2+}+\text{H}^+(\text{D}^+)$  as a function of collision energy. Also listed is the statistical uncertainty and total combined (statistical plus systematic) uncertainty estimated at the 90% confidence level (CL). See text for details.

| Collision energy (eV/u) | Cross section ( $10^{-16}$ cm $^2$ ) | Statistical uncertainty ( $10^{-16}$ cm $^2$ ) | Total uncertainty ( $10^{-16}$ cm $^2$ ) |
|-------------------------|--------------------------------------|--|--|
| $0.07^{+0.03}_{-0.02}$  | 65.8                                 | 4.8  | 9.2                                      |
| $0.11^{+0.04}_{-0.02}$  | 61.8                                 | 7.9  | 11                                       |
| $0.24^{+0.08}_{-0.04}$  | 48.0                                 | 9  | 11                                       |
| $0.38^{+0.11}_{-0.06}$  | 44.2                                 | 3.1  | 6.1                                      |
| $0.79\pm 0.05$          | 39                                   | 3.4  | 6.0                                      |
| 1.5                     | 48.5                                 | 2.3  | 6.0                                      |
| 3.5                     | 46.6                                 | 1.3  | 5.5                                      |
| 6.8                     | 46.1                                 | 2.6  | 6.1                                      |
| 10.8                    | 48.2                                 | 2.9  | 6.4                                      |
| 15.7                    | 47.6                                 | 2.5  | 6.2                                      |
| 22.0                    | 47.7                                 | 2.6  | 6.3                                      |
| 26.9                    | 41.7                                 | 2.3  | 5.9                                      |
| 35.8                    | 44.6                                 | 1.2  | 5.5                                      |
| 47.0                    | 43.1                                 | 1.2  | 5.3                                      |
| 70.0                    | 41.3                                 | 1.0  | 5.1                                      |
| 95.6                    | 40.2                                 | 1.1  | 5.0                                      |
| 161                     | 37.2                                 | 1.1  | 4.8                                      |
| 201                     | 31.4                                 | 1.3  | 4.0                                      |
| 302                     | 31.3                                 | 1.3  | 4.0                                      |
| 432                     | 31.2                                 | 0.7  | 3.8                                      |
| 600                     | 29.5                                 | 2.3  | 4.3                                      |
| 826                     | 33.5                                 | 1.8  | 4.4                                      |

the previous measurements had a significant fraction of metastables in their ion beams.

The MOCC calculation of Gargaud and McCarroll [11] is in good agreement with the current measurements and with those of Seim *et al.* for energies above 200 eV/u. The Gargaud and McCarroll results are significantly larger than the measurements of Huber and Can *et al.*, but in fair agreement with the present measurements, though slightly smaller, especially below 200 eV/u. Both the Gargaud and McCarroll calculation and the current measurements find that the cross section increases towards lower energies, contrary to the experimental findings of Huber and Can *et al.* The earlier MOCC calculations of Heil *et al.* [12] at lower energies are in very good agreement with the current measurement even suggesting a hint of the measured dip near 1 eV/u.

The present MOCC calculations show reasonable agreement with the present measurements above  $\sim 1$  eV/u. Our MOCC results are typically 25% smaller than the experimental data from  $\sim 1$  up to  $\sim 100$  eV/u, and as much as 20% larger than the present measurements between 100 and 1000 eV/u. At lower energies, where the MOCC calculations suggest a significant target isotope effect, the difference approaches a maximum factor of  $\sim 2.5$ . The discrepancies are likely related to errors incurred by digitization of the

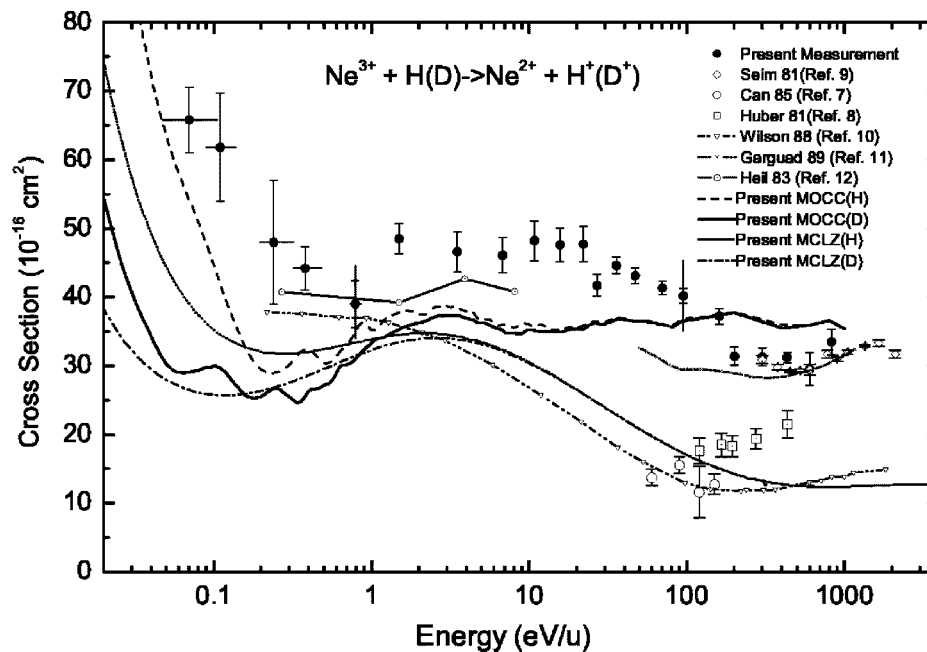


FIG. 3. Ion-atom merged-beam measurements and MOCC and MCLZ calculations of the electron-capture cross section for  $\text{Ne}^{3+} + \text{H}(\text{D})$  as a function of collision energy. Previous experiment and theory are also shown. The statistical errors (estimated at a 90% confidence level) of the present measurements are shown, except at energies 0.79 and 95.6 eV/u, where both the relative and total errors are shown at a 90% confidence level. For collision energies less than 1 eV/u the uncertainties in center-of-mass collision energy are also shown by horizontal lines. See text for details.

diabatic potential data. However, the MOCC calculations do confirm that the cross section is generally flat at low energies with a significant rise with decreasing energy below  $\sim 0.4\text{--}1$  eV/u. The MOCC calculations indicate a significant isotope effect at low energies.

As with the MCLZ calculations of Wilson *et al.* [10], the current MCLZ calculations underestimate the measurements. However, the onset and magnitude of a target isotope effect is similar to the MOCC results. Agreement of the MCLZ calculations of Wilson *et al.* [10] with the data of Can *et al.* is likely to be fortuitous as discussed by Gargaud and McCarroll [11] who suspected that a systematic error exists in choosing the curve crossing parameters used in the MCLZ calculations. However, our MCLZ results are very similar to those of Wilson *et al.*, though we used the Butler-Dalgarno [29] empirical couplings, while Wilson *et al.* used those of Taulbjerg [32]. The discrepancy with the measurements is more likely dominated by the neglect of nonlocal interactions in the Landau-Zener approximation, which become important at higher energies.

Consideration of the state-selective cross sections can give some insight into the behavior of the total cross section. The relative state-selective measurements of Wilson *et al.* [10], which were normalized with their MCLZ calculations, show that from 100 to 1000 eV/u the capture to the  $2s^2 2p^3 3p$  configuration decreases while capture to the  $2s^2 2p^3 3s$  configuration increases with increasing collision energy. This is generally consistent with both sets of MCLZ calculations and the current MOCC calculations which are shown in Fig. 4 for collisions with D. The decrease in this energy range in the  $3p^3 P$  and  $3p^5 P$  channels is not as pronounced in the MOCC results compared to the MCLZ

calculations (not shown). The flat behavior in the total MOCC cross section between  $\sim 3$  and 1000 eV/u is due to the relatively flat behavior of the  $3p^3 P$ ,  $3p^5 P$ , and  $3s^3 D^0$  capture channels. The drop in the measured cross section from 1.5 eV/u to the minimum at 0.8 eV/u followed by the Langevin-like  $1/v$  rise at lower energies is seen qualitatively to be a consequence of the sudden drop in the  $3p^5 P$  channel below 3 eV/u in the MOCC calculations and the steep in-

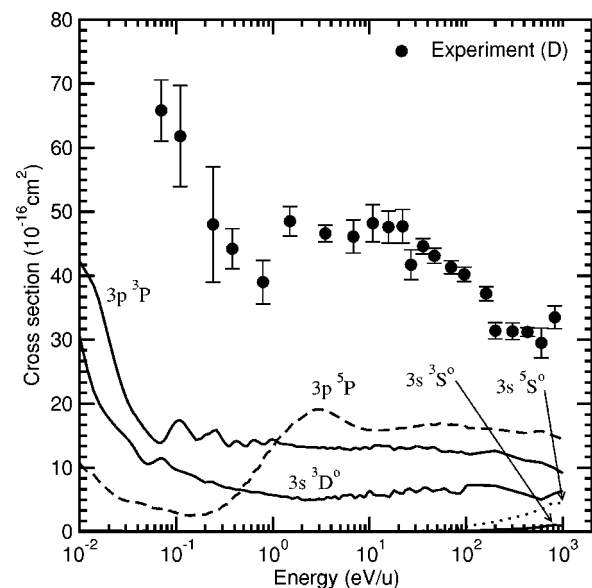


FIG. 4. State-selective MOCC cross sections for  $\text{Ne}^{3+} + \text{D} \rightarrow \text{Ne}^{2+} (2p^3 3l^3, 5L) + \text{D}^+$  in comparison with the current measured total cross section from Fig. 3.

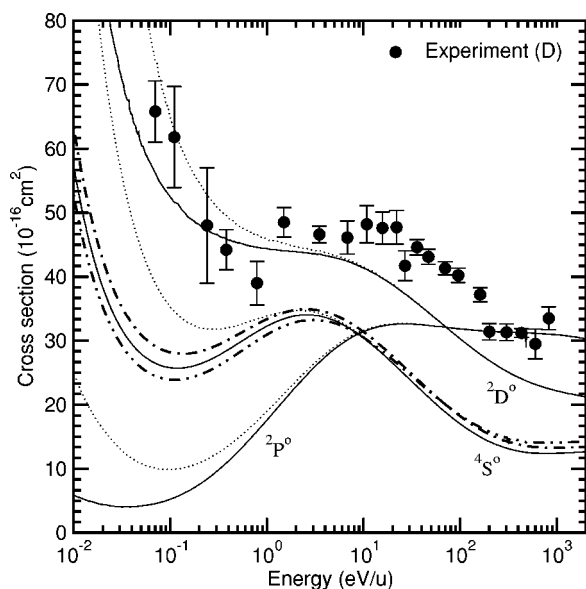


FIG. 5. MCLZ cross sections for  $\text{Ne}^{3+} + \text{H(D)}$  electron capture for ground state  $\text{Ne}^{3+}(^4S^0)$  and metastable  $\text{Ne}^{3+}(^2P^0)$  and  $\text{Ne}^{3+}(^2D^0)$  ions: H target (dotted lines), D target (solid lines). The sum of ground state and metastable ions are given for 91%  $^4S^0$ , 9%  $^2P^0$ , and 0%  $^2D^0$  (thick dot-dash line) and 91%  $^4S^0$ , 0%  $^2P^0$ , and 9%  $^2D^0$  (thick dot-dot-dash line) for the D target in comparison to the current measured values from Fig. 3.

crease in capture to the  $3p\ ^3P$  and  $3s\ ^3D^0$  channels for  $E < 1$  eV/u. Apparently, quantitative agreement between experiment and theory will require more modern quantum chemistry calculations of the molecular potentials and couplings.

Finally, in Fig. 5 we give estimates of the metastable cross sections in comparison to the ground-state cross section using the MCLZ method for both H and D targets. As illustrated in Fig. 3, the MCLZ method can only give a qualitative picture of the expected magnitudes and energy dependencies. The MCLZ calculations demonstrate, however, that the metastable  $\text{Ne}^{3+}(^2D^0)$  and  $\text{Ne}^{3+}(^2P^0)$  cross sections are within factors of 2–3 of the ground-state cross section and their presence in reasonable fractions should not affect the measured cross sections for the ground state adversely. As for the ground state, the metastable cross sections reveal a significant target isotope effect for energies less than  $\sim 1$  eV/u. To estimate the influence of the metastables in the ion beam, we consider the D target and the lower limit of the ground-state fraction, 91%, as measured by electron-impact

ionization from Sec. III B. We then delegate the remaining 9% to either the  $\text{Ne}^{3+}(^2D^0)$  or  $\text{Ne}^{3+}(^2P^0)$  ions and plot the summed cross sections in Fig. 5. The dispersion is within the uncertainties of the measurements, though there does appear to be a slight tendency to enhance the measured cross sections for  $E \gtrsim 10$  eV/u. Therefore, metastable contamination of the ion beam is not expected to significantly decrease the reliability of the measured cross sections for the ground  $\text{Ne}^{3+}$  state.

## V. CONCLUSIONS

Using a merged-beam setup, we have measured absolute total electron-capture cross sections for  $\text{Ne}^{3+}$  on D for the collision energy range of 0.07–826 eV/u. MOCC and MCLZ calculations have been performed for collisions with both H and D for energies from 0.01 to 1000 eV/u. The present MOCC calculations are typically smaller than the present measurements by 25–40%, particularly at low energies where the MOCC results predict a significant isotope effect. The discrepancy grows with decreasing energy and is likely due to errors introduced in digitizing the molecular potentials of Heil *et al.* [12]. This is suggested by the very good agreement of the MOCC calculations of Heil *et al.*, between 0.3 eV/u and 8 eV/u, with the merged-beam measurements. Modern quantum chemistry calculations are needed to improve the MOCC calculations. Above 200 eV/u, the current measurements show good agreement with the previous measurements of Seim *et al.* [9] and the previous MOCC calculations of Gargaud and McCarroll [11].

## ACKNOWLEDGMENTS

This work was supported by the Division of Chemical Sciences, Office of Basic Energy Sciences, U.S. Department of Energy and the Division of Applied Plasma Physics, Office of Fusion Energy Sciences, U.S. Department of Energy, Contract No. DE-AC05-00OR22725 with UT-Batelle, LLC, and by the NASA SARA program under Work Order No. 10,060 with UT-Batelle, LLC. C.V.J. was supported by the Chemical Sciences, Geosciences and Biosciences Division, Office of Basic Energy Sciences, Office of Science, U.S. Department of Energy. J.G.W. and P.C.S. acknowledge support from NASA Grant No. NAG5-11453 and helpful discussions with Professor T. G. Heil. D.W.S. was supported in part by the NASA Space Astrophysics Research & Analysis Grant No. NAG5-5420 and NSF Galactic Astronomy Program No. 0307203.

- [1] H. D. Gilbody, *Adv. At. Mol. Phys.* **22**, 143 (1986).  
 [2] W. P. West, B. Goldsmith, T. E. Evans, and R. E. Olson, in *Atomic and Molecular Data and Their Applications*, edited by D. R. Schultz, P. S. Krstić, and F. Ownby, AIP Conf. Proc. No. 636 (AIP, Melville, NY, 2002), p. 171.  
 [3] G. A. Shield, A. Dalgarno, and A. Sternberg, *Phys. Rev. A* **28**, 2137 (1983).

- [4] M. Pena and S. Torres-Peimbert, *Rev. Mex. Astron. Astrofis.* **11**, 35 (1985).  
 [5] R. E. S. Clegg, J. P. Harrington, and P. J. Story, *Mon. Not. R. Astron. Soc.* **221**, 61 (1986).  
 [6] G. Steigman, *Astrophys. J., Lett. Ed.* **195**, L39 (1975).  
 [7] B. A. Huber, *Z. Phys. A* **299**, 307 (1981).  
 [8] C. Can, T. J. Gray, S. L. Varghese, J. M. Hall, and L. N.

- Tunnell, Phys. Rev. A **31**, 72 (1985).
- [9] W. Seim, A. Müller, I. Wirkner-Bott, and E. Salzborn, J. Phys. B **14**, 3475 (1981).
- [10] S. M. Wilson, R. W. McCullough, and H. B. Gilbody, J. Phys. B **21**, 1027 (1988).
- [11] M. Gargaud and R. McCarroll, J. Phys. (Paris), Colloq. **50**, C1-127 (1989).
- [12] T. G. Heil, S. E. Butler, and A. Dalgarno, Phys. Rev. A **27**, 2365 (1983).
- [13] C. C. Havener, F. W. Meyer, and R. A. Phaneuf, in *Physics of Electronic and Atomic Collisions*, edited by W. R. McGillivray, I. E. McCarthy, and M. C. Standage (AIP, New York, 1992), p. 381.
- [14] C. C. Havener, in *Accelerator-Based Atomic Physics Techniques and Applications*, edited by S. M. Shafroth and J. C. Austin (AIP, New York, 1997), p. 117.
- [15] M. Pieksma, M. Gargaud, R. McCarroll, and C. C. Havener, Phys. Rev. A **54**, R13 (1996).
- [16] P. C. Stancil and B. Zygelman, Phys. Rev. Lett. **75**, 1495 (1995).
- [17] C. C. Havener, M. S. Huq, H. F. Krause, P. A. Schulz, and R. A. Phaneuf, Phys. Rev. A **39**, 1725 (1989).
- [18] C. C. Havener, M. S. Huq, F. W. Meyer, and R. A. Phaneuf, J. Phys. (Paris), Colloq. **50**, C1-7 (1989).
- [19] F. W. Meyer, M. E. Bannister, J. W. Hale, C. C. Havener, O. Woitke, and Q. Yan, in *Proceedings of the 13th International Workshop on ECR Ion Sources*, edited by D. P. May and J. E. Ramirez (Texas A & M University, College Station, TX, 1997), p. 102.
- [20] T. W. Imai, M. Kimura, J. P. Gu, G. Hirsch, R. J. Buenker, J. G. Wang, P. C. Stancil, and L. Pichl, Phys. Rev. A **68**, 012716 (2003).
- [21] D. C. Gregory, F. W. Meyer, A. Müller, and P. Defrance, Phys. Rev. A **34**, 3657 (1986).
- [22] M. E. Bannister, Phys. Rev. A **54**, 1435 (1996).
- [23] S. Bashkin and J. O. Stoner, Jr., *Atomic Energy Levels and Grotrian Diagrams* (North-Holland, Amsterdam, 1975), Vol. 1, p. 315.
- [24] W. Lotz, Z. Phys. **261**, 241 (1968).
- [25] N. Djurić, M. E. Bannister, A. M. Derkatch, D. C. Griffin, H. F. Krause, D. B. Popović, A. C. H. Smith, B. Wallbank, and G. H. Dunn, Phys. Rev. A **65**, 052711 (2002).
- [26] M. Kimura and N. F. Lane, Adv. At., Mol., Opt. Phys. **26**, 79 (1990).
- [27] B. Zygelman, D. L. Cooper, M. J. Ford, A. Dalgarno, J. Gerratt, and M. Raimondi, Phys. Rev. A **46**, 3846 (1992).
- [28] B. R. Johnson, J. Comput. Phys. **13**, 445 (1973).
- [29] S. E. Butler and A. Dalgarno, Astrophys. J. **241**, 838 (1980).
- [30] R. K. Janev, D. S. Belić, and B. H. Brandsen, Phys. Rev. A **28**, 1293 (1983).
- [31] A. Mroczkowski, D. W. Savin, R. Rejoub, P. S. Krstić, and C. C. Havener, Phys. Rev. A **68**, 032721 (2003).
- [32] K. Taulbjerg, J. Phys. B **19**, L367 (1986).